Effect of higher heating rate during continuous annealing on microstructure and mechanical properties of cold-rolled 590 MPa dual-phase steel

Yonggang Deng, Hongshuang Di[a], Jiecen Zhang, and Liqing Chen

State Key Laboratory of Rolling and Automation, Northeastern University, 3-11 Wenhua Road, Shenyang 110819, China

Abstract. In this presentation, the effect of higher heating rate in continuous annealing on microstructure and mechanical properties of a cold-rolled 590 MPa ferrite-martensite dual-phase steel were investigated by using microstructural observation and mechanical property measurement. The results show that compared with the conventional continuous annealed steels heated at a rate of 5 °C/s (CA), the average ferrite grain sizes heated at a higher rate (300 °C/s, HRA) was obviously refined from 15.6 μm to 5.3 μm. The morphology of martensite is observed to shift from network along ferrite grain boundaries to uniformly dispersed in the final DP590 microstructure. Twinned substructure of martensite can be found when heated at a higher heating rate in continuous annealing. EBSD orientation maps show that the fraction of low angle grain boundary is increased in HRA sample compared to CA sample. The HRA sample has excellent mechanical properties when compared to the CA sample. The variations of strength, elongation, strain hardening behavior and fracture mechanism of the this DP590 steel with different heating routine were further discussed in relation to microstructural features.

1. Introduction

Dual phase (DP) steels are low-carbon and low-alloy steels with 10–30 vol.% of martensite and a ductile ferrite matrix, which are widely used in the automotive industry because of the good combination of high strength and good formability at low production cost [1, 2]. DP steels are characterized by a continuous yielding behavior with a low initial flow stress and a high initial work hardening rate [3, 4]. Through careful control of the chemistry and heat treatment path, dual-phase steel with different microstructure, or different mechanical properties, can be obtained [5–7].

Recently, higher heating rate during continuous annealing treatment have received much attention to produce ferrite-martensite DP steels. In the case of rapid heating during continuous annealing, ferrite recrystallization is strongly suppressed during the heating stage, while the austenite formation and its distribution are strongly influenced by overlapping of the processes of recrystallization and austenitization and thus it could refine the grain structure, to improve both strength and ductility at
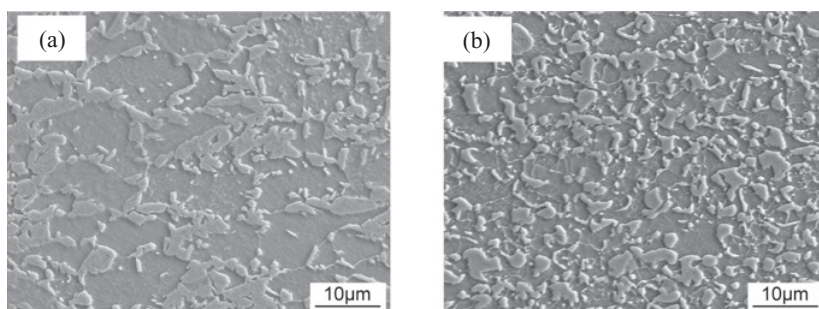
[a] Corresponding author: dhshuang@mail.neu.edu.cn

Figure 1. SEM micrographs showing microstructures in annealed dual-phase steel with varying heating rate. CA-5 °C/s (a), and HRA-300 °C/s (b).

the same time [8]. The purpose of this study was to explore the influence of higher heating rate on the microstructure and tensile behavior of DP590 steel. The strain hardening behavior and fracture mechanisms were also studied in this presentation.

2. Experimental

An industrial Fe-0.08C-0.42Si-1.83Mn-0.16P-0.18Cr (wt.%) cold-rolled low carbon steel sheet with an initial thickness of 1.5 mm was investigated in the present study.

In order to study the effect of higher heating rate on the microstructures and mechanical properties of DP steel, the samples were annealed at inter-critical region (820 °C/60s) with different heating rate (5 °C/s and 300 °C/s) followed by water-quenching to form a DP microstructure.

To characterize the microstructure, the samples were grounded and then polished. After polishing, the samples were etched with a 4 vol% nital solution for 10 s. The etched samples were used for observing the microstructure by means of scanning electron microscope (SEM) on a FEI Quanta 600. The transmission electron microscopy (TEM) was carried out using FEI Tecnai G2F20S-TWIN microscope. FEI Quanta 600 scanning electron microscope (SEM) with an OIM 4000 EBSD was used to analysis the grain boundary characteristics of annealed samples.

After inter-critical annealing, tensile samples according to GB T228-2002 standard were cut from the heated-treated steel. Tensile samples with a nominal gauge length of 50 mm and nominal width of 12.5 mm were used. The tensile test was carried out at across head speed of 3 mm/min using a 100 kN Instron tensile machine. All specimens were tested to failure. During the tensile experiments, force and displacement plots were recorded, from which stress and strain data was obtained.

3. Results and discussion

3.1 Microstructural evaluation

The microstructures of the heat-treated samples are shown in Fig. 1. It is evident that both treatments resulted in ferrite-martensite DP microstructure, however, the morphology, size and distribution of martensite phase varied significantly with the heat-treatment schedules. Compared with Fig. 1(a) with a heating rate of 5 °C/s, the sample with higher heating rate (300 °C/s) have a fine grain structure and martensite uniformly dispersed in the final DP microstructure. According to a quantitative measurement by image-pro-plus, the amount of martensite in HRA sample was increased from 23% to 27%, while the ferrite grain sizes was obviously refined to 5.3 μm from 15.6 μm as compared with the conventional heating rate of 5 °C/s in continuous annealing process.
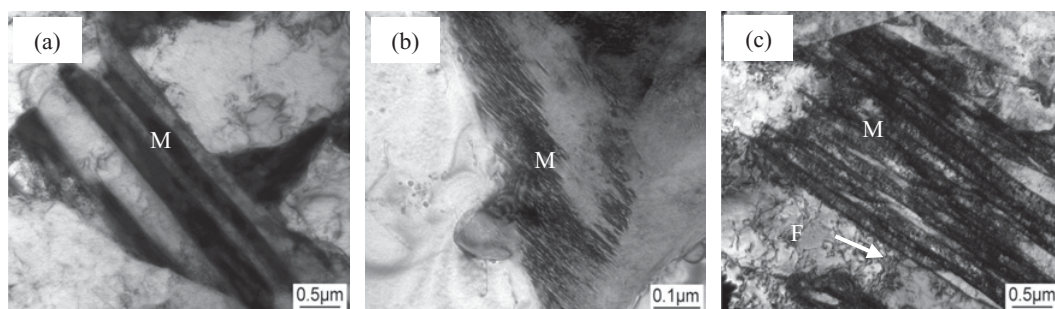
Figure 2. TEM micrographs of the annealed dual-phase steel heated with varying rate. Lath of martensite in CA sample (a), twin of martensite in HRA sample (b) and lath of martensite in HRA sample (c). F: Ferrite; M: Martensite.
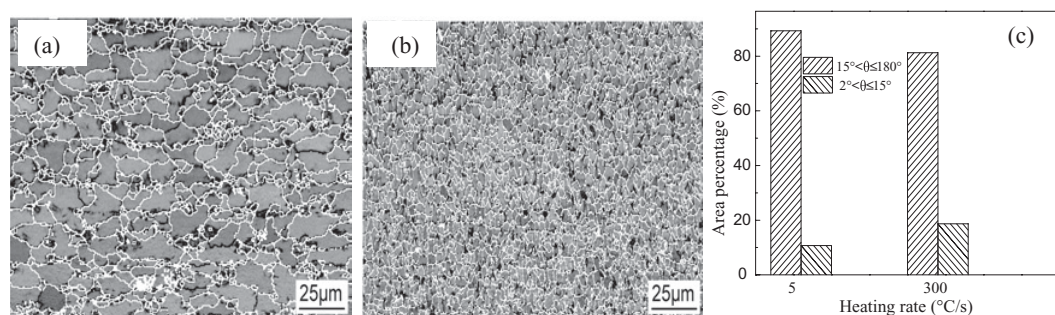

Figure 3. EBSD misorientation images of the annealed dual-phase steel heated with varying rate. CA-5 °C/s (a), HRA-300 °C/s (b) (white grain boundaries $15° < \theta \leq 180°$, black grain boundaries $2° < \theta \leq 5°$), and misorientation between adjacent grains (c) measured from (a) and (b).

Figure 2(a) show the TEM images of CA sample, where the martensite shows coarse lath-like feature and a few dislocations can be seen in the vicinity of martensite. However, in the case of HRA sample, the martensite shows two typical substructure (lath and twin) and higher dislocation density in ferrite matrix can be observed as marked by white arrow in Fig. 2(c).

Figure 3(a) and (b) show the EBSD orientation images and Fig. 3(c) shows the distribution misorientation between adjacent grains measured from Fig. 3(a) and (b). The fraction of low angle grain boundary was increased from 10.7% to 18.7% with the increase of heating rate. It is known that low angle boundary is beneficial for the plastic and toughness of metal.

To understand the effect of higher heating rate on the microstructure of ferrite-martensite dual-phase steels, it's useful to consider the processing history of initial microstructure of steel. The received steel had been cold-rolled and inter-critical annealing followed by water quenching. An important consideration is austenite spatial distribution and content at the end of the inter-critical annealing cycle will be inherited into the final microstructures after quenching.

In the case of CA sample, the ferrite recrystallization would fully complete when heated to the inter-critical zone and then austenite nucleation at recrystallization ferrite grain boundaries and grows along them [9, 10]. In addition, at lower heating rate, there are sufficient time for ferrite and austenite grains to grow which produce larger ferrite and martensite grain.

In the case of HRA sample, the time from recrystallize start temperature (660 °C, measured by quantitative metallography) to inter-critical annealing temperature (820 °C) is very short, only 0.53 s, which means that the ferrite have no time to recrystallize prior to reaching the inter-critical
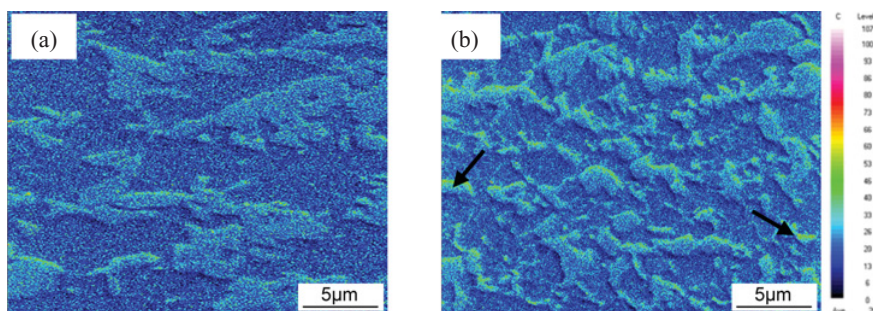
Figure 4. EPMA images of the annealed dual-phase steel heated with rates of CA-5 °C/s (a) and HRA-300 °C/s (b).
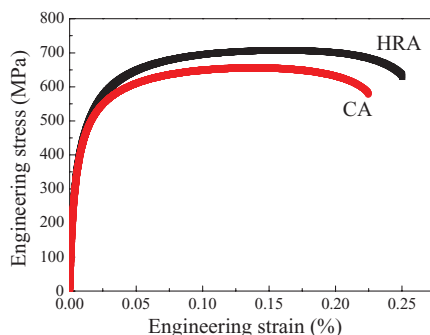

Figure 5. Engineering stress-strain curves of dual-phase steel with varying heating rate.

temperature. In the unrecrystallized sample, carbide particles distributed along deformed ferrite grain boundary which provides an increased nucleation density compared with the fully recrystallized samples [11]. Subsequently, the austenite grows rapidly until they cover almost all the deformed ferrite grain boundaries and at the same time the ferrite recrystallization occurs. The overlapping between ferrite recrystallization and austenitization during annealing could refine the grain sizes. The amount of austenite nuclei increases with the heating rate and rapid annealing could refine the grain sizes, the more amount of austenite could also produce more martensite.

Figure 4(a) and (b) presents the distribution of carbon in annealed samples. Martensite is the mainly rich carbon region, while, CA sample shows more uniform distribution than HRA sample. In the case of HRA sample, higher carbon rich region can be observed as black arrowed in Fig. 4(b). This can be attributed to the fact that a higher heating rate cause uneven distribution of carbon, in these regions twin substructure of martensite could be produced.

3.2 Mechanical properties

Typical engineering stress-strain curves obtained from the tensile testing of the DP steel samples subjected to different heating rate are presented in Fig. 5. Both curves show clear discontinuous yielding characters of DP steel. Mechanical properties of different DP samples are summarized in Table 1. It can be seen that HRA sample exhibit higher strengths and elongation. Compared with the CA sample, the average yield strength $R_{p0.2}$ of HRA sample increases from 335 MPa to 351 MPa (4.7% higher), the ultimate tensile strength R_m improves from 655.5 MPa to 706 MPa (4.7% higher), the total elongation is enhanced from 22.4% to 25.0% (11.6% higher) and its uniform elongation from 13.8% to 15.4% (11.6% higher).

Table 1. Mechanical properties of the investigated steel after continuous annealing with varying heating rate.

HR (°C/s)	Rp0.2 (MPa)	Rm (MPa)	UEL (%)	TEL (%)	Rm× TEL (MPa %)
5	335	656	13.8	22.4	14683
300	351	706.0	15.4	25.0	17650

In general, the enhancement in strength is accompanied by a deterioration of elongation [4]. However, this does not apply to present study. This can be reflected in the strain hardening ability and the fracture mechanisms of the steels.

3.2.1 Strain hardening behavior

A study in Ref. [12] showed that the modified C-J analysis method based on Swift equation can describe the multistage strain hardening behavior, as expressed in Eq. (1):

$$\varepsilon = \varepsilon_0 + k\sigma^m. \tag{1}$$

Differentiating the above equation with respect to ε, we have the Eq. (2) in logarithmic form:

$$\ln(d\sigma/d\varepsilon) = (1 - m)\ln\sigma - \ln(km) \tag{2}$$

where σ and ε are true stress and true strain, respectively, k is the constants which are normally called the strength coefficient, ε_0 is the maximum elastic strain, $(1-m)$ is the slope. It can be seen that the work hardening ability decreases with the increase of the values of $(1-m)$ since σ is an independent variable. The plots of $\ln(d\sigma/d\varepsilon)$ versus $\ln\sigma$ for both the samples are shown in Fig. 6, also the values of $(1-m)$ for both stages in Fig. 6.

Analysis of strain-hardening ability of the generated DP microstructures by modified C-J technique resulted into only two stages of strain-hardening irrespective of the heating rates as shown in Fig. 6. Two stages of strain hardening have been demonstrated earlier for DP steels [13].

The lower slope in the first stage of both samples, indicating higher strain hardening is related to the ferrite deformation restrained by the martensite. The second stage with higher slope, indicating lower strain hardening ability, is due to the co-deformation of both ferrite and martensite [14]. However, compared with CA sample, the HRA sample shows higher strain hardening ability in both stages. This can be attributed to the fine grain structure and uniformly martensite distribution. Saeidi et al. [15] reported, during the transformation from austenite to martensite by quenching, volume expansion lead to geometrically necessary dislocation (GNDs) generation along the ferrite/martensite interfaces in the ferrite grains. So the higher these interfaces in the fine grain sample, the higher density of geometrically necessary dislocation present in the microstructure and the higher the strain hardening ability. In addition, Balliger et al. [16] found that the strain hardening rate of DP steels increases with a decrease in the martensite island size. Furthermore, uniformly martensite distribution lead to reduction of strain partitioning between ferrite and martensite, thus, the strain hardening ability was greatly improved.

A higher strain hardening rate delays the onset of necking and therefore, increases the uniform elongation, this consistent with the measurement results in Table 1.

3.2.2 Fracture mechanism

The fracture surfaces of the investigated specimens are shown in Fig. 7. The fracture surfaces reveal mixture of cleavage facets and dimples for both the specimens. However, the area of the cleavage surfaces in the HRA sample is lower than the CA sample. It was observed that the size of dimples in HRA sample is finer than CA sample. The reason for this phenomenon can be attributed to the random and uniform disperse of martensite in ferrite matrix which restrict the growth of micro-voids.
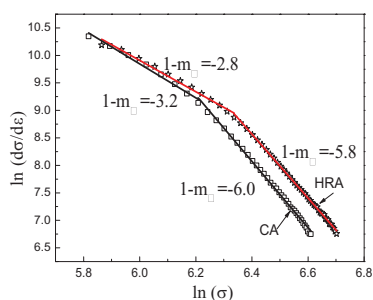
Figure 6. Modified C-J plot of ln(dσ/dε) versus ln(σ) of annealed samples with varying heating rate.
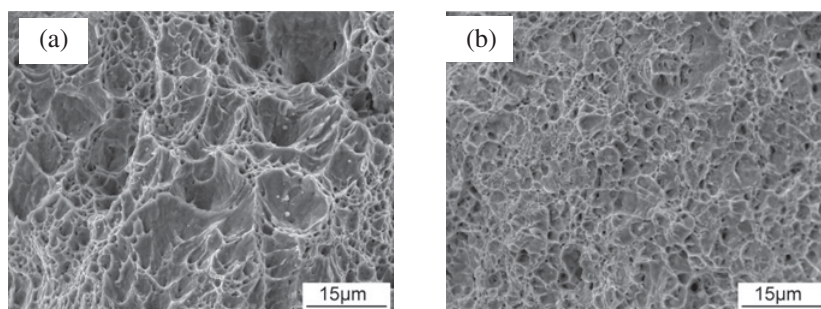

Figure 7. SEM micrograph on the fracture surfaces of annealed samples with different heating rate (a) CA-5 °C/s and (b) HRA-300 °C/s.

Some researchers [13, 17] have shown that large, banded and interconnected martensite islands in DP steels, compared to the fine and isolated martensite particles, result in weaker fracture properties. They observed that interconnected martensite distributed along ferrite grain boundaries cracked easily and the fracture mode was predominantly cleavage type. While martensite cracking was less frequent and the micro-voids were smaller and micro-voids density were higher in the specimen with fine martensite particles and form the fracture was dimple depression type.

4. Conclusions

For DP590 steel, a good combination of strength and ductility can be achieved by rapid heating process, and the work-hardening ability is also increased. Compared with the conventional heating rate (5 °C/s) in continuous annealing process, the ultimate tensile strength is improved from 656 MPa to 706 MPa and the total elongation is enhanced from 22.4% to 25.0% after processed by rapid heating. In such a case, the average ferrite grain in sample with higher heating rate was obviously refined to 5.3 μm from about 15.6 μm, and the martensite morphology was changed into fine and uniformly dispersed in the final microstructure from network along ferrite grain boundaries. Twinned substructure of martensite occurred when heated at a higher heating rate in continuous annealing.

References

[1]   R.O. Rocha, T.M.F. Melo, E.V. Pereloma, D.B. Santos, Mater. Sci. Eng. A **391**, 296 (2005)
[2]   G. Avramovic-Cingara, Y. Ososkov, M.K. Jain, D.S. Wilkinson, Mater. Sci. Eng. A **516**, 7 (2009)
[3]   H. Ghassemi-Armaki, R. Maaß, S.P. Bhat, J.R. Greer, K.S. Kumar, Acta Mater. **62**, 197 (2014)

[4] Y. Sun, X.F. Li, X.Y. Yu, D.L. Ge, J. Chen, J.S. Chen, Acta Metall. Sin. (Engl. Lett.) **27**, 101 (2014)

[5] A. Fallahi, Mater. Sci. Tech. **22**, 81 (2002)

[6] A. Bag, K.K. Ray and E.S. Dwarakadasa, Metall. Mater. Trans. A **30**, 1193 (1999)

[7] D. Das and P.P. Chattopadhyay, J. Mater. Sci. **44**, 2957 (2009)

[8] C. Lesch, P. Plvarez, W. Bleck, J.G. Sevillano, Metall. Mater. Trans. A **38**, 188 (2007)

[9] J. Huang, W.J. Poole, and M. Militzer, Metall. Mater. Trans. A **35**, 3363 (2004)

[10] P. Li, J. Li, Q.G. Meng, W.B. Hua, D.C. Xu, J. Alloy. Compd. **578**, 320 (2013)

[11] R.R. Mohantv, O.A. Girina, N.M. Fonstein, Metall. Mater. Trans. A **42**, 3680 (2011)

[12] V. Colla, M.D. Sanctis, A. Dimatteo, Metall. Mater.Trans. A **40**, 2557 (2009)

[13] Z. Jiang, J. Lian, Z. Guan, Mater. Sci. Eng. A **190**, 55 (1995)

[14] A. Kumar, S.B. Singh, K.K. Ray, Mater. Sci. Eng. A **474**, 270 (2008)

[15] N. Saeidi, F. Ashrafizadeh, B. Niroumand, Mater. Sci. Eng. A **599**, 145 (2014)

[16] N.K. Balliger, T. Gladman, Met. Sci. **15**, 95 (1981)

[17] M. Mazinani, W.J. Poole, Metall. Mater. Trans. A **38**, 328 (2007)